Scientia Iranica C (2021) 28(3), 1366–1377

Sharif University of Technology
Scientia Iranica
Transactions C: Chemistry and Chemical Engineering
http://scientiairanica.sharif.edu

Triple-enzymatic activity of $CuMn_2O_4$ nanoparticles: Analytical applications for H_2O_2 and L-cysteine detection

M. Rahnamabaghy, A. Fallah Shojaei*, and Z. Moradi-Shoeili

Department of Chemistry, Faculty of Sciences, University of Guilan, Rasht, P.O. Box 1914, Iran.

Received 19 December 2019; received in revised form 12 August 2020; accepted 8 February 2021

KEYWORDS
Peroxidase;
Oxidase;
Catalase;
$CuMn_2O_4$;
H_2O_2;
L-cysteine.

Abstract. $CuMn_2O_4$ nanoparticles (NPs) were prepared via a co-precipitation method and characterized using microscopic and spectroscopic analyses. $CuMn_2O_4$ NPs exhibit a triple-enzymatic activity including peroxidase-, oxidase- and catalase-like activity. The effect of various parameters on the initial rate of the catalytic reaction of $CuMn_2O_4$ NPs with peroxidase- and oxidase-like activity was studied by UV-vis spectroscopy following the increasing absorption at 415 nm corresponding to the oxidation product of substrate *o*-phenylenediamine (OPD). Kinetic analyses indicate the Michaelis-Menten model for $CuMn_2O_4$ NPs for both peroxidase- and oxidase-like activity. Based on the high peroxidase-like activity of $CuMn_2O_4$ NPs, they were further studied as a colorimetric sensor for the detection of H_2O_2 with a linear range from 0.5 mM to 22 mM, and a detection limit of 0.11 mM. Inhibition of the high oxidase-like activity of $CuMn_2O_4$ NPs was utilized for colorimetric detection of L-cysteine with a linear range from 50 μM to 200 μM, and a detection limit of 54.15 μM.

1. Introduction

Peroxidases and oxidases form a subcategory of a large group of enzymes called oxidoreductases. They catalyze the transfer of electrons from one molecule as an electron donor to another as an electron acceptor, in oxido-reduction reactions. Peroxidases and oxidases act on H_2O_2 and O_2 as an electron acceptor, respectively [1]. The use of natural enzymes is limited due to their structural complexity, low stability, high cost of preparation and purification, and substrate specificity [2,3]. After the pioneering work of Yan et al. on the peroxidase-like activity of Fe_3O_4 [4], many nanomaterials have been reported for mimicking enzymatic activity in order to overcome the natural enzymes' drawbacks [5–9]. Nanomaterials with enzymatic activity are divided into several categories such as carbon-based [10–12], metal-based [13–16], metal oxide-based [17–19] and metal sulfide-based [20,21]. In addition, bi- and multi-metallic nanoparticles (NPs) [22,23], mixed metal oxide NPs [24,25], and nanocomposites, in which metal or metal oxides are combined with other types of nanomaterials [26,27], are also rapidly developed for their synergistic effects. Enzymatic activity of nanomaterials has been used in many applications from biosensing, immunoassay, neuroprotection, cancer diagnosis and therapy to pollutant removal [6,28–30].

In these typical reactions, the oxidation of substrate catalyzed by peroxidase-mimetic nanomaterials is usually used for fabrication of sensors or biosensors in

*. *Corresponding author. Tel.: +98 1333362207*
E-mail addresses: rahnamabaghy@gmail.com (M. Rahnamabaghy); a-fallah@guilan.ac.ir (A. Fallah Shojaei); zmoradi@guilan.ac.ir (Z. Moradi-Shoeili)

doi: 10.24200/sci.2021.55071.4059

order to detect H_2O_2 and H_2O_2-related analytes, such as glucose, cholesterol, xanthine and etc. [26,31,32]. Also, sensors or biosensors can fabricate based on the inhibition of peroxidase- and/or oxidase-like activity, which is usually used for the detection of metals, biothiols, antioxidants, etc. [33–36].

Mixed metal oxides in a spinel structure with the formula AB_2O_4 (A is bivalent and B is trivalent metal ions) have attracted enormous interest among inorganic-based nanomaterials because of their special electrochemical properties, high catalytic activities and exceptional chemical stability [37]. Gao et al. have fabricated hollow $MnCo_2O_4$ nanofibers with excellent oxidase-like activity in the oxidation of $3,3',5,5'$-Tetramethylbenzidine (TMB). They used the inhibition effect of sulfite and L-cysteine on oxidase-like activity for the detection of these species [24]. Vetr et al. reported the peroxidase-like catalytic activity of MFe_2O_4 (M = Mn, Co, Ni, Zn) [38] and mesoporous $MnCo_2O_4$ [39] in the chromogenic oxidation of OPD to OPDox, which were used for detection of H_2O_2. Ferrites (MFe_2O_4) and cobaltites (MCo_2O_4) (M is bivalent metal ions) have been studied for their peroxidase and oxidase-like activities [24,25,31,35,36,38–43], but little attention has been paid to enzymatic activity of manganites (MMn_2O_4). In this study, $CuMn_2O_4$ NPs were prepared via a co-precipitation method without any surface modification, characterized by typical techniques, and their enzymatic activity was studied. Results showed that $CuMn_2O_4$ NPs can catalyze the oxidation of OPD both in the presence of H_2O_2 and O_2, in a similar way to the action of peroxidase- and oxidase enzymes, respectively. The catalase-like activity of $CuMn_2O_4$ NPs was monitored by the decomposition reaction of H_2O_2 into oxygen and water. Also, the kinetics and mechanism of peroxidase- and oxidase-like activity were investigated. Based on the peroxidase-like activity of $CuMn_2O_4$ NPs, a simple colorimetric sensor for H_2O_2 detection, and based on the oxidase-like activity of $CuMn_2O_4$ NPs, a simple and sensitive colorimetric sensor for L-cysteine detection, were established.

2. Experimental section

2.1. Materials

$Cu(CH_3COO)_2.3H_2O$, $Mn(CH_3COO)_2.4H_2O$, Na_2CO_3, NaOH, Citric Acid (CA), Na_2HPO_4, H_2O_2 30%, *o*-phenylenediamine (OPD) were purchased from Sigma-Aldrich or Merck and used as received without further purification. Deionized water was used throughout the experiments.

2.2. Characterization

Powder X-Ray Diffraction (XRD) data were collected with a Philips PW 1830 diffractometer (Cu-Kα X-radiation, λ = 1.54 Å). The Scanning Electron Microscopy (SEM) image was taken using a KYKY-EM3200 scanning electron microscope. The elemental analysis was recorded with an Energy Dispersive X-ray (EDX) analyzer, MIRA3 FEG-SEM series. The FT-IR spectra of the sample in the form of a KBr pellet were recorded using an Alpha-Bruker FT-IR spectrophotometer. All absorbance measurements were recorded with a RAYLEIGH (UV-1800) ultraviolet-visible (UV-vis) spectrometer. The O_2 generation from H_2O_2 decomposition was recorded by a portable water quality meter (Model: 8603, S/N: 1000258).

2.3. Preparation of $CuMn_2O_4$ NPs

$CuMn_2O_4$ NPs were prepared via the co-precipitation procedure [44]. In this procedure, $Cu(CH_3COO)_2.H_2O$ (0.49 g, 2.5 mmol) and $Mn(CH_3COO)_2.4H_2O$ (1.22 g, 5 mmol) were dissolved in 10 mL distilled water. The mixture was gradually diluted to 50 mL. To achieve precipitate, the solution was maintained at 60–80°C and pH was raised to about 8 by dropwise addition of sodium carbonate (2M) for 10 min. The precipitate was aged under constant conditions (80°C, pH 8, 150 rpm stirring) for 2 h. The precipitate was then filtered, and washed with boiling distilled water and alcohol to bring the pH of the sub-filtration to 7. The black precipitate was dried in vacuum for 16 h and calcined at 415°C for 2 h.

2.4. Study of triple-enzymatic activity of $CuMn_2O_4$ NPs

To study peroxidase-like activity, H_2O_2 (30%, 50 μL) was added into a solution of OPD (10 mM) and the mixture was diluted to 5 mL. Then, a 0.5 mL dispersed solution of $CuMn_2O_4$ NPs (100 μg/mL) was added. For investigating the oxidase-like catalytic activity, $CuMn_2O_4$ NPs (100 μg/mL) was added into a fresh solution of OPD (10 mM) in the absence of H_2O_2, and the mixture was diluted to 5 mL. In the above two studies, the absorbance was recorded in the wavelength range from 350 nm to 500 nm with a time interval for 30 s up to 10 min at room temperature. To investigate the catalase-like activity of $CuMn_2O_4$ NPs, H_2O_2 (30%, 50 μL) and $CuMn_2O_4$ NPs (100 μg/mL) solutions were added into 5 mL distilled water. The concentration of O_2 generated from H_2O_2 decomposition was recorded by a dissolved oxygen meter.

The steady-state kinetic analysis of peroxidase- and oxidase-like activity of $CuMn_2O_4$ NPs was studied using UV-vis detection for 200 s in a kinetic scan mode. The reaction was carried out at room temperature and the absorbance measurements at 415 nm were performed immediately after the aqueous solution containing the desired concentrations of H_2O_2 and OPD mixed with the optimum content of $CuMn_2O_4$ NPs (120 μg/mL) and the optimum pH of the buffer

solution (pH 6.2). The kinetic analysis of peroxidase-like activity of $CuMn_2O_4$ NPs was performed with optimum concentration of OPD (15 mM) and varied concentration of H_2O_2 (0.5–40 mM) as substrate, or vice versa optimum concentration of H_2O_2 (8 mM) and varied concentration of OPD (1–24 mM) as a substrate, in the final volume of the reaction mixture with 3 mL of buffer solution. Similarly, the kinetic analysis of the oxidase-like activity of $CuMn_2O_4$ NPs was performed with a fixed concentration of oxygen soluble and varied concentration of OPD (1–20 mM) as a substrate, in the final volume of the reaction mixture of 3 mL buffer solution. Then, the reaction rates were determined from the concentration versus time plots using the Lambert-Beer law ($A = \varepsilon bc$ where, A: Absorbance, ε: molar extinction coefficient, b: optical path length, and c: concentration of substrate) in the initial stage of the catalytic reaction. The kinetic parameters were determined by the typical Michaelis-Menten equation:

$$V_0 = V_{\max}[S]/(K_m + [S]),$$

where V_0 is the initial rate of reaction, $V_{\max}$ is the maximum reaction rate, K_m is the Michaelis constant and $[S]$ is the concentration of substrate. Ascorbic acid was used to identify the mechanism of the catalytic oxidation reaction of OPD by $CuMn_2O_4$ NPs in the presence or absence of H_2O_2.

2.5. Colorimetric detection of H_2O_2

A typical colorimetric analysis was realized as follows: different concentrations of H_2O_2 (0.5–32 mM) were added into mixtures of a fresh solution of OPD (15 mM) in buffer solution (pH 6.2). A dispersed solution of $CuMn_2O_4$ NPs (120 μg/mL) was added and the mixture was incubated at room temperature for 10 min. Then, H_2SO_4 was added into the mixture to stop the reaction. Finally, the absorbance measurements for OPDox at 415 nm of yellowish-brown solutions were carried out. The Limit Of Detection (LOD) was calculated by data analysis from the slope of a calibration curve.

2.6. Colorimetric detection of L-cysteine

In this detection, different concentrations of L-cysteine (0–400 μM) were added into mixtures of fresh solutions of OPD (40 mM) in the mentioned buffer solution (pH 6.2). Then, a dispersed solution of $CuMn_2O_4$ NPs (120 μg/mL) was added. The mixture was incubated at room temperature for 3 min. Then, the absorbance measurements at 388 nm of brownish pale green solutions were carried out. The LOD was calculated by data analysis from the slope of a calibration curve. For selectivity study and to investigate the effect of other amino acids, a stock solution (1 mM) of 5 kinds of natural amino acids including arginine, glycine, methionine, tryptophan, and tyrosine were added under the same conditions.

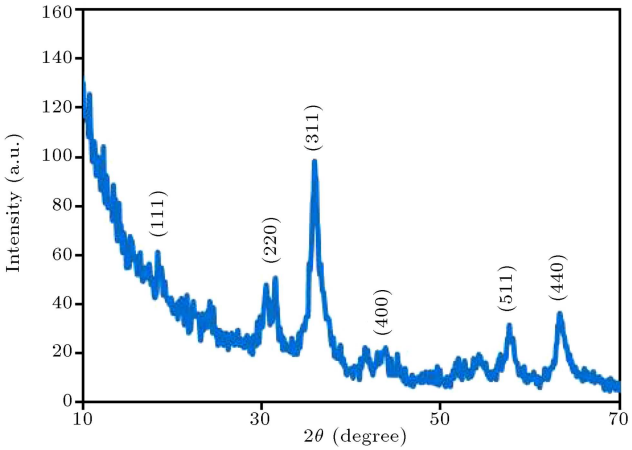

Figure 1. X-Ray Diffraction (XRD) pattern of $CuMn_2O_4$ nanoparticles (NPs).

3. Results and discussion

3.1. Characterization

The structure of the as-prepared catalyst was determined by powder XRD. The XRD pattern in the range of 2θ = 10-80° is shown in Figure 1. The peaks in the 2θ = 18.3°, 31.4°, 35.8°, 43.9°, 54.2°, 58.1°, and 63.5° are corresponded to (111), (220), (311), (400), (422), (511), and (440) planes, in a cubic crystal structure, respectively. These results confirm the spinel structure of $CuMn_2O_4$ NPs with high purity, as in previous studies [24,35,44]. The particle size of $CuMn_2O_4$ NPs was estimated using the most intense peak (311) based on the Debye-Scherrer equation [45] ($D = k\lambda/\beta\cos\theta$ where, D: average crystalline size, k: Scherrer constant (0.89), λ: X-ray wavelength used, β: the angular line width at half maximum intensity, and θ is the Bragg's angle in degree units), and was found to be about 5 nm.

Figure 2 shows the FT-IR spectrum of the as-prepared $CuMn_2O_4$ NPs. The absorption bands around 400–600 cm^{-1} are related to the oxygen coordinated with metal ions (Cu^{2+} and Mn^{3+}) [46]. The absorption peaks at 3437 and 1637 cm^{-1} are related to the vibration of O-H of water molecules adsorbed on the surface of the particles [39].

The morphology and size of the as-prepared catalyst were characterized by SEM. The SEM image in Figure 3(a) shows that the $CuMn_2O_4$ NPs have spherical shapes with an average diameter of about 30–80 nm. A moderate degree of agglomeration was also observed in the SEM images. The EDX is used to measure the composition of participates, which verified that $CuMn_2O_4$ NPs contain copper, manganese, and oxygen without any impurities, as shown in Figure 3(b).

3.2. The triple-enzymatic catalytic activity of $CuMn_2O_4$ NPs

To study the peroxidase-like activity of $CuMn_2O_4$ NPs in the presence of H_2O_2, OPD was used as a donor

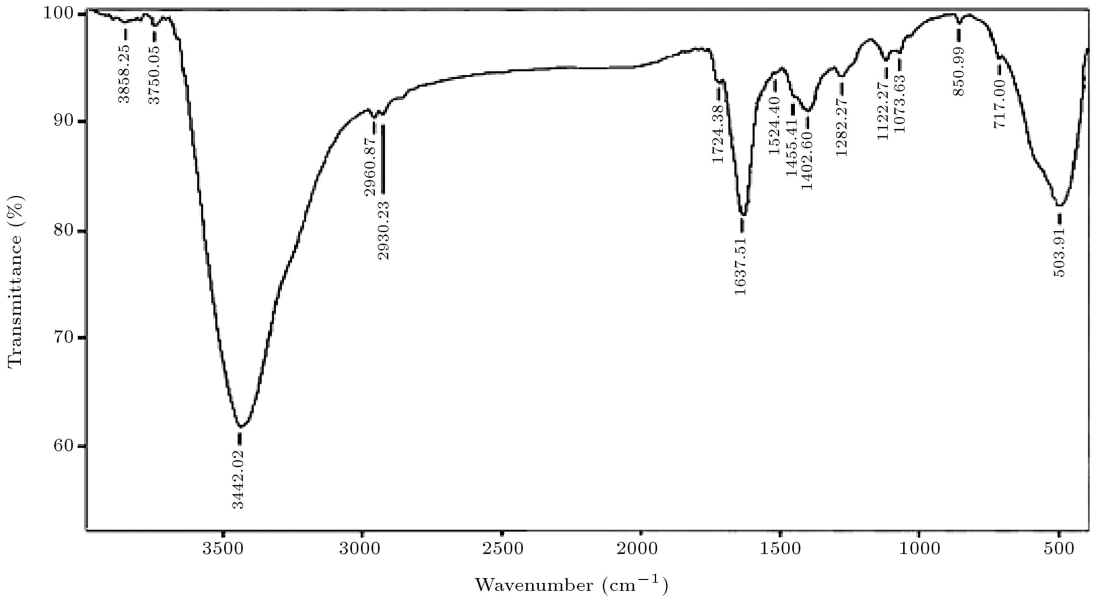

Figure 2. FT-IR spectrum of $CuMn_2O_4$ nanoparticles (NPs).

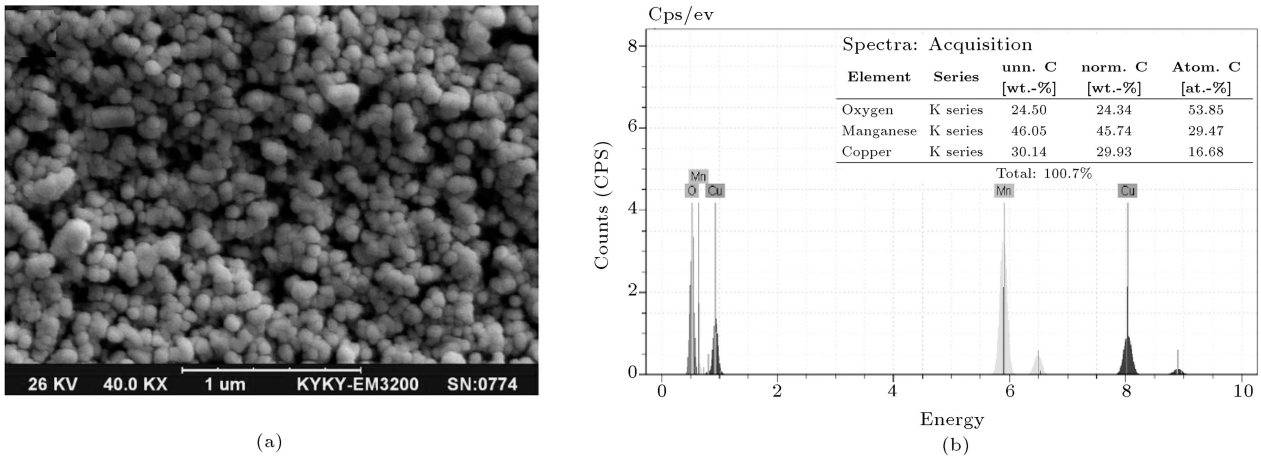

Figure 3. Scanning Electron Microscopy (SEM) image (a) and Energy Dispersive X-ray (EDX) spectrum (b) of $CuMn_2O_4$ nanoparticles (NPs).

substrate. $CuMn_2O_4$ NPs can also oxidase OPD by dissolved oxygen. In two cases, a new band at 410–415 nm produced OPDox that could be observed by the naked eye [47,48]. The control reaction in the absence of $CuMn_2O_4$ NPs showed little variation in the absorbance at 410–415 nm (Figure 4(a)). There was more absorbance from OPDox in peroxidase-like activity than there was in the oxidase-like activity of $CuMn_2O_4$ NPs, as shown in Figure 4(a). Furthermore, $CuMn_2O_4$ NPs can catalyze the decomposition of H_2O_2 to produce O_2 as bubbles, which could also be observed in the mixture solution of $CuMn_2O_4$ NPs and H_2O_2 (Figure 4(b)).

3.3. Optimization

Several factors, such as time, pH, $CuMn_2O_4$ NPs content, H_2O_2, and OPD concentration should be considered in the oxidation reaction study of OPD by $CuMn_2O_4$ NPs with peroxidase- or oxidase-like activity. The effect of pH was measured by incubating the suspension of $CuMn_2O_4$ NPs in the pH of a buffer solution from 3 to 7. A significant absorbance was observed from the supernatant solution in the leach test, when the pH value of the buffer solution was around 3–5, which would be evidence that the NPs are unstable in acidic pH conditions, and leached cations from $CuMn_2O_4$ NPs into the solution can oxidase the OPD. As shown in Figure 5(a), the oxidation reaction has a higher rate when the pH value of the buffer solution is around 3–5. Under the optimal pH 6.2, the peroxidase-like activity was enhanced directly with the increasing content of $CuMn_2O_4$ NPs at a constant concentration of OPD and H_2O_2 (Figure 5(b)).

As $CuMn_2O_4$ NPs can oxidase OPD before adding

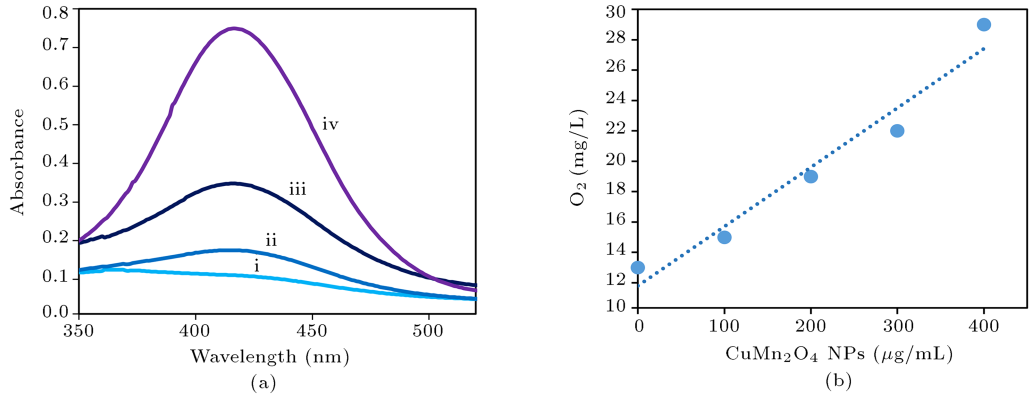

Figure 4. The absorbance measurement for OPDox in the wavelength range from 350 nm to 500 nm in different reaction systems: (a) i: OPD (10 mM); ii: OPD (10 mM)+H_2O_2 (30%, 50 μL); iii: OPD (10 mM) + $CuMn_2O_4$ NPs (100 μg/mL); iv: OPD (10 mM) + H_2O_2 (30%, 50 μL) + $CuMn_2O_4$ NPs (100 μg/mL and (b) dependence of dissolved oxygen generation of catalase-like activity of $CuMn_2O_4$ NPs on $CuMn_2O_4$ NPs content. Conditions: H_2O_2 (30%, 50 μL) and citric acid-Na_2HPO_4 buffer solution (pH 6.2).

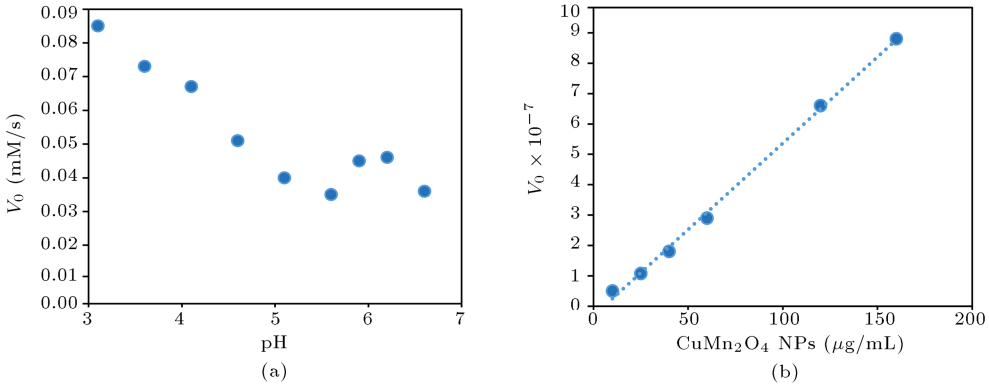

Figure 5. Dependence of the enzymatic activity of $CuMn_2O_4$ nanoparticles (NPs) on (a) pH (dispersed solution of $CuMn_2O_4$ NPs (120 μg/mL), H_2O_2 (8 mM), and OPD (15 mM)) and (b) $CuMn_2O_4$ NPs content (H_2O_2 (8 mM), OPD (15 mM), and citric acid-Na_2HPO_4 buffer solution (pH 6.2)).

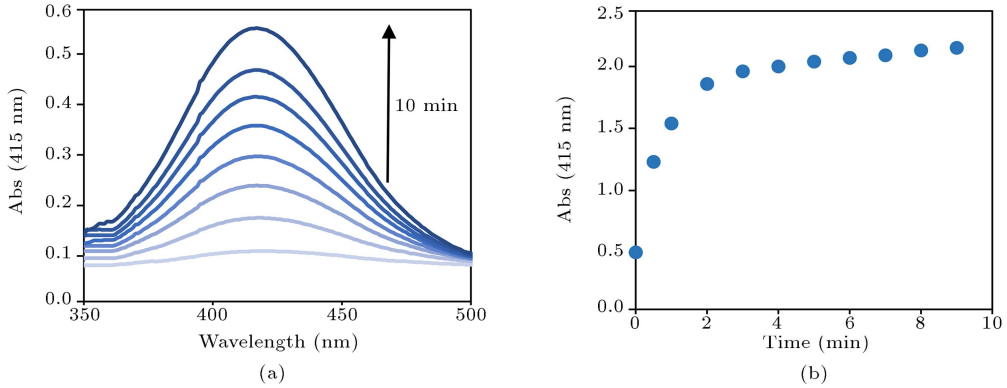

Figure 6. The absorbance measurement for OPDox in (a) the wavelength ranges from 350 nm to 500 nm for 10 min and (b) a kinetic scan mode at 415 nm. Conditions: H_2O_2 (8 mM), OPD (15 mM), dispersed solution of $CuMn_2O_4$ NPs (120 μg/mL), and citric acid-Na_2HPO_4 buffer solution (pH 6.2).

H_2O_2 with oxidase-like activity and can decompose H_2O_2 before adding OPD with catalase-like activity, it is important that the reagents be added in the order already mentioned. As shown in Figure 6(a), the absorbance at 415 nm was increasing with the reaction time. The absorbance versus time plot shown in Figure 6(b) indicated that the absorbance related to OPDox increased gradually and reached a maximum at 200 s, then, fixed with little variation in the absorbance.

The optimal conditions for the maximum

peroxidase-like catalytic activity of prepared $CuMn_2O_4$ NPs during the oxidation process including $CuMn_2O_4$ NPs content, H_2O_2, and OPD concentrations were set as 120 μg/mL, 8 mM, 15 mM, respectively.

3.4. Kinetic and mechanism analysis of peroxidase- and oxidase-like activities of $CuMn_2O_4$ NPs

Steady-state kinetics were carried out to study the effect of each substrate concentration on the reaction rate, to achieve kinetic parameters and to investigate the reaction mechanism. To calculate the initial reaction rate, absorbance was converted to the corresponding concentration of OPDox using the Lambert-Beer law and related to the molar extinction coefficient of OPDox value $\varepsilon = 16700\ M^{-1}cm^{-1}$ (at 415 nm) [36]. Figure 7(a)–(d) shows the steady-state kinetic analysis of the oxidation reaction of OPD by $CuMn_2O_4$ NPs in the presence of H_2O_2. As shown in Figure 7(a) and (c), reaction rates were found to be dependent on the concentrations of H_2O_2 and OPD and increased gradually with increasing the concentrations of H_2O_2 and OPD. The reactions reached a maximum rate to saturation of the reactivity of $CuMn_2O_4$ NPs [36]. The K_m and V_{max} values for each OPD and H_2O_2 substrates were calculated using the Lineweaver-Burk plots of the double reciprocal of the Michaelis-Menten equation. The $CuMn_2O_4$ NPs possess higher peroxidase-like activity in oxidation of OPD compared to that of the natural Horseradish Peroxidase (HRP) enzyme [18], as well as those corresponding single metal oxides, CuO [49–51] and MnO_2 [18] with the K_m and V_{max} value of 0.08 mM and 10.8 mMs^{-1}, toward OPD, and 0.59 mM and 16.9 mMs^{-1} toward H_2O_2, respectively (Table 1).

The kinetic of oxidase-like activity of $CuMn_2O_4$ NPs was investigated, as earlier described, for peroxidase activity. The kinetic parameters, K_m and V_{max}, were found to be 0.199 mM and 5.63 mMs^{-1} toward OPD, respectively (Figure 8(a) and (b)).

Furthermore, the mechanism of enzymatic (peroxidase and oxidase)-like activity of $CuMn_2O_4$ NPs was studied using ascorbic acid as a radical scavenger [52,53]. As shown in Figure 9, the absorption at 410–415 nm indicates the production of OPDox, which confirms $CuMn_2O_4$ NPs can oxidase OPD in the presence of H_2O_2 despite using ascorbic acid as a radical

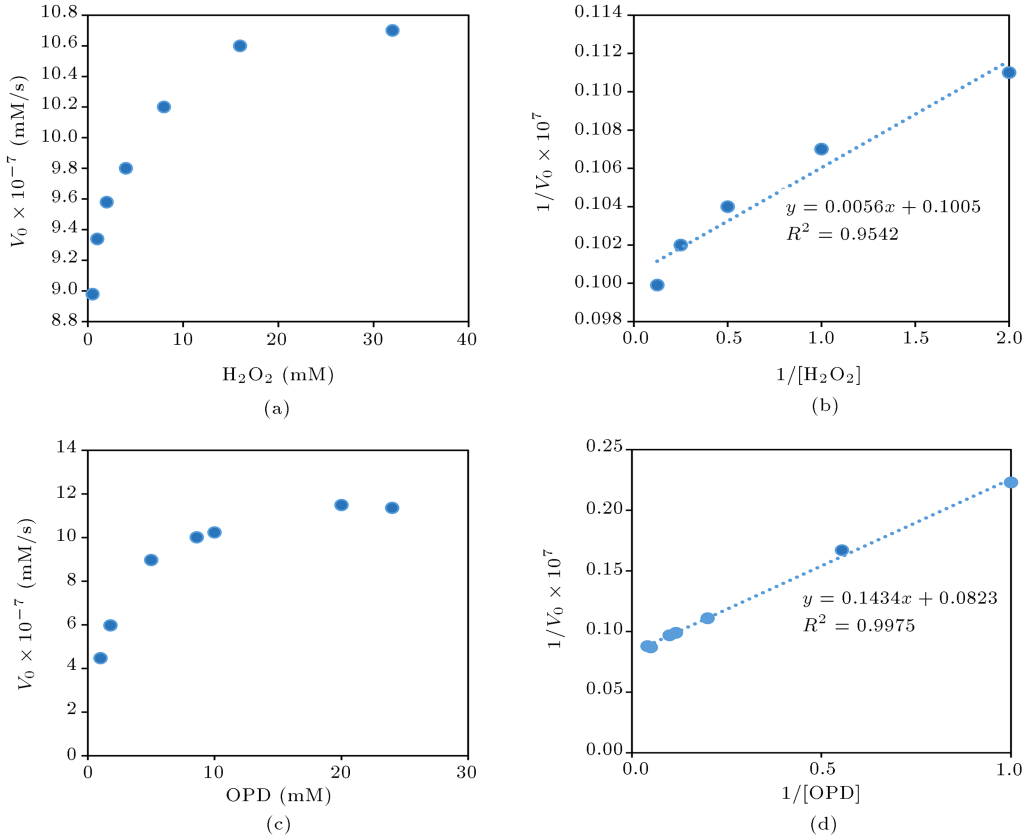

Figure 7. The steady-state kinetic analysis of oxidation reaction of OPD by $CuMn_2O_4$ nanoparticles (NPs) in the presence of H_2O_2: (a) The concentration of OPD was optimum (15 mM) and the H_2O_2 concentration was varied (0.5–40 mM), (b) lineweaver-Burk plots of peroxidase-like activity of $CuMn_2O_4$ NPs in varied concentration of H_2O_2, (c) the concentration of H_2O_2 was optimum (8 mM) and the OPD concentration was varied (1–24 mM), and (d) lineweaver-Burk plots of peroxidase-like activity of $CuMn_2O_4$ NPs in varied concentration of OPD. Conditions: Dispersed solution of $CuMn_2O_4$ NPs (120 μg/mL) and citric acid-Na_2HPO_4 buffer solution (pH 6.2).

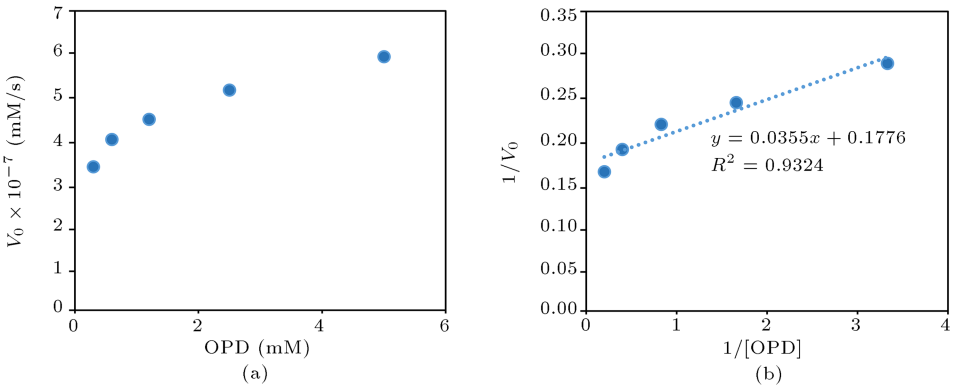

Figure 8. The steady-state kinetic analysis of oxidation reaction of OPD by $CuMn_2O_4$ nanoparticles (NPs) in absence of H_2O_2 (a–b): (a) The OPD concentration was varied (0–5 mM) and (b) lineweaver-Burk plot of peroxidase-like activity of $CuMn_2O_4$ NPs with different concentrations of OPD. Conditions: Dispersed solution of $CuMn_2O_4$ NPs (120 μg/mL) and citric acid-Na_2HPO_4 buffer solution (pH 6.2).

Table 1. Comparison of kinetic parameters for substrate oxidation by inorganic-based nanomaterials with peroxidase-like activity.

		H_2O_2				
Catalyst	**Substrate**	K_m **(mM)**	$V_{max} \times 10^{-7}$ **(Ms^{-1})**	K_m **(mM)**	$V_{max} \times 10^{-7}$ **(Ms^{-1})**	**Ref.**
HRP	OPD	0.6	0.46	0.34	0.94	[18]
HRP	TMB	0.43	0.1	3.7	0.87	[35]
BSA-MnO_2	OPD	0.31	0.82	0.12	0.57	[18]
$MnFe_2O_4$	OPD	27	1.04	—	—	[39]
CuO NPs	TMB	0.013	—	85.6	—	[49]
CuO nanosheets	TMB	—	—	15.8	0.077	[50]
CuO/Pt	TMB	0.41	1.46	2.88	0.88	[51]
$CuMn_2O_4$ NPs	OPD	0.08	10.8	0.59	16.9	This work

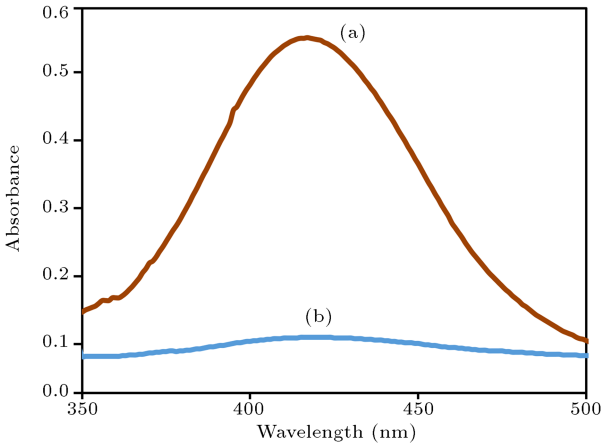

Figure 9. The absorbance measurement for OPDox in the wavelength range from 350 nm to 500 nm in the presence of ascorbic acid and: (a) with H_2O_2 and (b) without H_2O_2.

scavenger. This can be because the mechanism of the peroxidase-like activity of $CuMn_2O_4$ NPs is different from that of Fenton or Fenton-like reactions, which are related to the formation of free radicals from H_2O_2. Therefore, $CuMn_2O_4$ NPs as a mediator can facilitate the electron transfer process from absorbed OPD on the surface of the $CuMn_2O_4$ NPs to H_2O_2 directly. A similar mechanism has been suggested previously for Co_3O_4 [25] and $NiCo_2O_4$ [54]. Also, ascorbic acid was used in the oxidation reaction of OPD by $CuMn_2O_4$ NPs with oxidase-like activity. Figure 10(b) shows no band at 410–415 nm, which indicates OPD oxidation by $CuMn_2O_4$ NPs did not occur in the presence of ascorbic acid. This result indicates ascorbic acid has an inhibition effect on the oxidation reaction of OPD on the $CuMn_2O_4$ NPs surface in the absence of H_2O_2 [36].

3.5. Colorimetric detection of H_2O_2 based on peroxidase-like activity of $CuMn_2O_4$ NPs

Detection of H_2O_2 as a by-product of several biochemical reactions or as a contaminant in various branches of industry has attracted enormous interest [55]. There are many types of analysis method for the detection and measurement of H_2O_2 [56,57]. Since the chromogenic oxidation of OPD to OPDox in a peroxidase-like activity system is dependent on H_2O_2 concentration, it can be used to determine the concentration

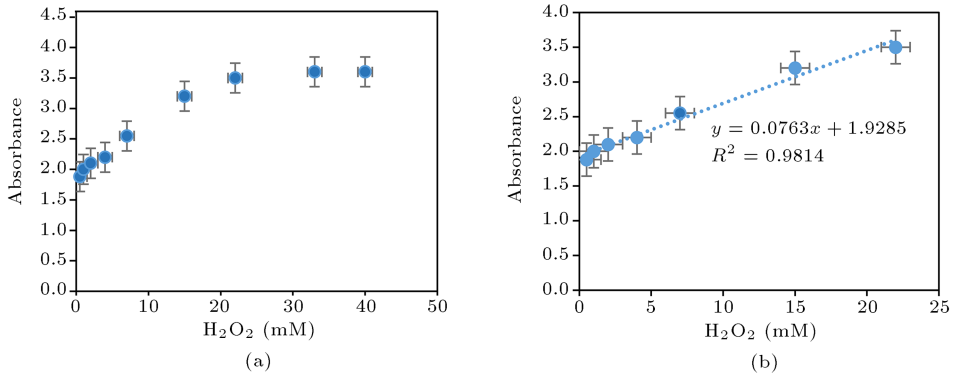

Figure 10. (a) The absorbance measurement for OPDox at 415 nm in the presence of H_2O_2 at different concentrations (0–40 mM). (b) Linear calibration plot for H_2O_2 determination using $CuMn_2O_4$ NPs.

Table 2. Comparison of the various peroxidase-like activities of inorganic-based nanomaterials for the detection of H_2O_2.

Catalyst	Substrate	Detection limit (mol/L)	Linear range (mol/L)	Ref.
$MnCo_2O_4$	OPD	2×10^{-4}	$5 \times 10^{-4} - 0.12$	[38]
$MnFe_2O_4$	OPD	0.3×10^{-4}	$1 \times 10^{-4} - 0.015$	[39]
CuS	OPD	0.11×10^{-6}	$1 \times 10^{-6} - 1 \times 10^{-3}$	[48]
$NiCo_2O_4$	TMB	0.21×10^{-6}	$1 \times 10^{-5} - 4 \times 10^{-4}$	[54]
$CuMn_2O_4$	OPD	1.1×10^{-4}	$5 \times 10^{-4} - 0.022$	This work

of H_2O_2 in aqueous solution as a simple analysis method. In Figure 10(a), the absorbance at 415 nm for oxidized OPD increases with the concentration of H_2O_2. Figure 10(b) shows the corresponding linear calibration curve. The linear range is from 0.5 mM to 22 mM, and the detection limit is calculated to be 0.11 mM. Table 2 gives a comparison of the detection limit and efficiency of the peroxidase-like activity of $CuMn_2O_4$ to oxidase OPD in the detection of H_2O_2 with other catalytic systems reported in the literature. These results show that the detection limit for the $CuMn_2O_4$/OPD system is the same order of magnitude as that of metal oxide nanoparticles such as mesoporous $MnCo_2O_4$.

3.6. Colorimetric detection of L-cysteine concentration based on the oxidase-like activity of $CuMn_2O_4$ NPs

The normal concentration of cysteine in plasma samples from healthy human subjects is approximately in the range of 200–300 μM [58]. Deficiency or unnatural levels of cysteine can directly cause slowed growth, liver damage, hair depigmentation, malabsorption syndromes, edema and lethargy [59,60]. There are many colorimetric detections of L-cysteine based on the peroxidase-like activity of inorganic-based nanomaterials [61–63], in which the high nucleophilicity of the thiol side chain in cysteine can decrease affinity toward the substrate by the shielding of $CuMn_2O_4$ NPs [33].

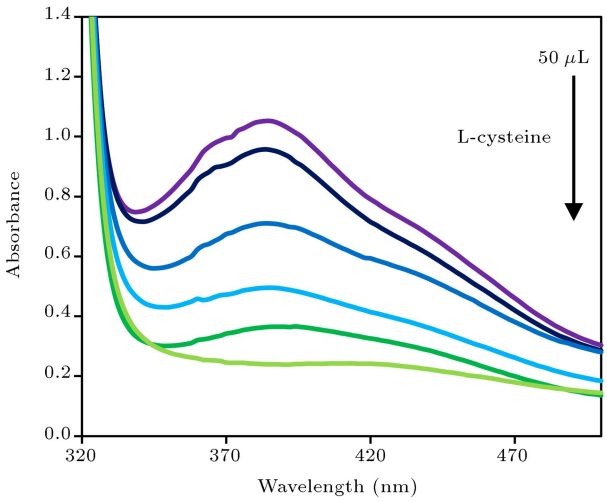

Figure 11. The absorbance measurement for OPDox in the wavelength range from 320 nm to 470 nm. Conditions: OPD (40 mM), dispersed solution of $CuMn_2O_4$ NPs (120 μg/mL), and citric acid-Na_2HPO_4 buffer solution (pH 6.2).

The colorimetric method for the detection of L-cysteine based on the oxidase-like activity of inorganic-based nanomaterials was also developed [24,64]. Figure 11 shows the absorbance measurement for OPDox in the oxidase-like activity system depending on L-cysteine concentration in the wavelength range from 320 nm to 470 nm. In Figure 12(a), the absorbance at 388 nm

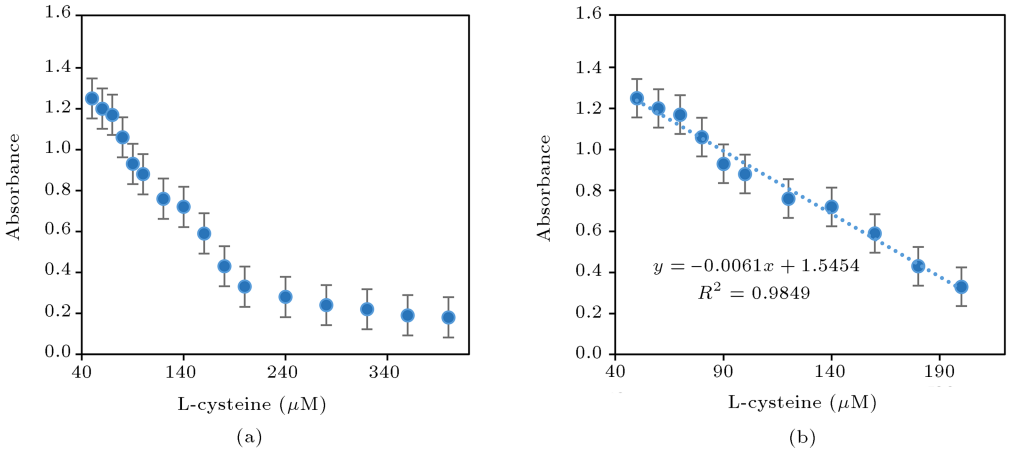

Figure 12. (a) The absorbance measurement for OPDox at 388 nm in the presence of L-cysteine at different concentrations (50–450 μM). (b) Linear calibration plot for L-cysteine determination using $CuMn_2O_4$ NPs.

Table 3. Comparison of various enzymatic activity of inorganic-based nanomaterials for the detection of L-cysteine.

Catalyst	Catalytic property	Substrate	Detection of limit (μmol/L)	Linear range (μmol/L)	Ref.
$MnCo_2O_4$	Oxidase-like	TMB	0.0343	0.5–10	[24]
$CuMnO_2$	Peroxidase-like	TMB	11.26	25–300	[61]
MoS_2-PPy-Pd	Peroxidase-like	TMB	0.08	1–10	[62]
Fe_3O_4	Peroxidase-like	TMB	0.028	2–10	[63]
Asp/Ce-NT	Oxidase-like	TMB	0.0332	0.08–10	[64]
$CuMn_2O_4$	Oxidase-like	OPD	56.15	50–200	This work

for OPDox decreases with an increasing concentration of L-cysteine. Figure 12(b) shows the corresponding linear calibration curve. The linear range is from 50 μM to 200 μM, and the detection limit is calculated to be 56.15 μM. The effect of other amino acids, including Arg, Gly, Met, Thr and Tyr, on OPD oxidation by $CuMn_2O_4$ NPs was also tested. As shown in Figure 13, the amino acids tested did not have a significant effect on the oxidase-like activity of $CuMn_2O_4$ NPs except L-cysteine. Compared with other inorganic-based nanomaterials with enzymatic activity for L-cysteine detection by UV-vis detection (Table 3), $CuMn_2O_4$ NPs possess high potential for the detection of L-cysteine in a wide range of concentration.

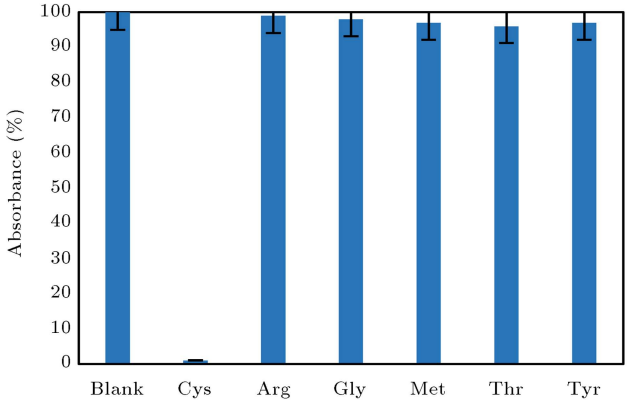

Figure 13. Changes of relative absorbance intensity at 415 nm in the OPD oxidation reaction catalyzed by $CuMn_2O_4$ nanoparticles (NPs) in the presence of 1 mM amino acids including Cys, Arg, Gly, Met, Thr, and Tyr.

4. Conclusions

This work investigated the triple-enzymatic activity of $CuMn_2O_4$ nanoparticles (NPs), including peroxidase-, oxidase- and catalase-like activity. A detailed analysis of the kinetic and mechanism by the UV-vis detection of the catalytic reaction confirms that $CuMn_2O_4$ NPs possess peroxidase-like activity superior to that of corresponding single metal oxides, which can be originated from transferring electrons from *o*-phenylenediamine (OPD) to H_2O_2 by $CuMn_2O_4$ NPs as mediator. Based on the peroxidase-like activity of $CuMn_2O_4$ NPs, a colorimetric method was developed for the detection of H_2O_2. Colorimetric detection of L-cysteine based on inhibition of the oxidase-like activity

of $CuMn_2O_4$ NPs was also developed, in which the affinity of $CuMn_2O_4$ NPs toward OPD decreases in the presence of L-cysteine. These results offer a simple, rapid, inexpensive and green method for analytical applications of $CuMn_2O_4$ as a versatile nanoparticle.

References

1. Champe, P.C., Harvey, R.A., and Ferrier, D.R., *Bio-Chemistry*, Lippincott Williams & Wilkins (2005).
2. Xie, J., Zhang, X., Wang, H., Zheng, H., and Huang, Y. "Analytical and environmental applications of nanoparticles as enzyme mimetics", *TrAC Trends in Anal. Chem.*, **39**, pp. 114–129 (2012).
3. Wulff G. "Enzyme-like catalysis by molecularly imprinted polymers", *Chem. Rev.*, **102**(1), pp. 1–28 (2002).
4. Gao, L., Zhuang, J., Nie, L., Zhang, J., Zhang, Y., Gu, N., Wang, T., Feng, J., Yang, D., Perrett, S., and Yan, X. "Intrinsic peroxidase-like activity of ferromagnetic nanoparticles", *Nature Nanotechnol.*, **2**(9), p. 577 (2007).
5. Ragg, R., Tahir, M.N., and Tremel, W. "Solids go bio: inorganic nanoparticles as enzyme mimics", *Europ. J. Inorg. Chem.*, **2016**(13–14), pp. 1906–1915 (2016).
6. Kuah, E., Toh, S., Yee, J., Ma, Q., and Gao, Z. "Enzyme mimics: advances and applications", *Chem. Eur. J.*, **22**(25), pp. 8404–8430 (2016).
7. He, W., Wamer, W., Xia, Q., Yin, J.J., and Fu, P.P. "Enzyme-like activity of nanomaterials", *J. Environ. Sci. Health C*, **32**(2), pp. 186–211 (2014).
8. Wei, H. and Wang, E. "Nanomaterials with enzyme-like characteristics (nanozymes): next-generation artificial enzymes", *Chem. Soc. Rev.*, **42**(14), pp. 6060–6093 (2013).
9. Chaibakhsh, N. and Moradi-Shoeili, Z. "Enzyme mimetic activities of spinel substituted nanoferrites (MFe_2O_4): A review of synthesis, mechanism and potential applications", *Mat. Sci. Eng. C*, **99**, pp. 1424–1447 (2019).
10. Cui, R., Han, Z., and Zhu, J.J. "Helical carbon nanotubes: intrinsic peroxidase catalytic activity and its application for biocatalysis and biosensing", *Chem. Europ. J.*, **17**(34), pp. 9377–9384 (2011).
11. Qu, F., Li, T., and Yang, M. "Colorimetric platform for visual detection of cancer biomarker based on intrinsic peroxidase activity of graphene oxide", *Biosens. Bioelectron.*, **26**(9), pp. 3927–3931 (2011).
12. Shi, W., Wang, Q., Long, Y., Cheng, Z., Chen, S., Zheng, H., and Huang, Y. "Carbon nanodots as peroxidase mimetics and their applications to glucose detection", *Chem. Commun.*, **47**(23), pp. 6695–6697 (2011).
13. Ma, M., Zhang, Y., and Gu, N. "Peroxidase-like catalytic activity of cubic Pt nanocrystals", *Colloids Surf. A*, **373**(1–3), pp. 6–10 (2011).
14. Jv, Y., Li, B., and Cao R. "Positively-charged gold nanoparticles as peroxidiase mimic and their application in hydrogen peroxide and glucose detection", *Chem. Commun.*, **46**(42), pp. 8017–8019 (2010).
15. Hu, L., Yuan, Y., Zhang, L., Zhao, J., Majeed, S., and Xu, G. "Copper nanoclusters as peroxidase mimetics and their applications to H_2O_2 and glucose detection", *Anal. Chim. Acta*, **762**, pp. 83–86 (2013).
16. Su, H., Liu, D.D., Zhao, M., Hu, W.L., Xue, S.S., Cao, Q., Le, X.Y., Ji, L.N., and Mao, Z.W. "Dual-enzyme characteristics of polyvinylpyrrolidone-capped iridium nanoparticles and their cellular protective effect against H_2O_2-induced oxidative damage", *ACS Appl. Mater. Interfaces*, **7**(15), pp. 8233–8242 (2015).
17. Liu, Y., Zhu, G., Bao, C., Yuan, A., and Shen, X. "Intrinsic Peroxidase-like Activity of Porous CuO Micro-/nanostructures with Clean Surface", *Chin. J. Chem.*, **32**(2), pp. 151–156 (2014).
18. Liu, X., Wang, Q., Zhao, H., Zhang, L., Su, Y., and Lv, Y. "BSA-templated MnO_2 nanoparticles as both peroxidase and oxidase mimics", *Analyst*, **137**(19), pp. 4552–4558 (2012).
19. Jiao, X., Song, H., Zhao, H., Bai, W., Zhang, L., and Lv, Y. "Well-redispersed ceria nanoparticles: promising peroxidase mimetics for H_2O_2 and glucose detection", *Anal. Methods*, **4**(10), pp. 3261–3267 (2012).
20. He, W., Jia, H., Li, X., Lei, Y., Li, J., Zhao, H., Mi, L., Zhang, L., and Zheng, Z. "Understanding the formation of CuS concave superstructures with peroxidase-like activity", *Nanoscale*, **4**(11), pp. 3501–3506 (2012).
21. Lin, T., Zhong, L., Guo, L., Fu, F., and Chen, G. "Seeing diabetes: visual detection of glucose based on the intrinsic peroxidase-like activity of MoS_2 nanosheets", *Nanoscale*, **6**(20), pp. 11856–11862 (2014).
22. Ding, Y., Yang, B., Liu, H., Liu, Z., Zhang, X., Zheng, X., and Liu, Q. "FePt-Au ternary metallic nanoparticles with the enhanced peroxidase-like activity for ultrafast colorimetric detection of H_2O_2", *Sens. Actuators B., Chem.*, **259**, pp. 775–783 (2018).
23. He, W., Wu, X., Liu, J., Hu, X., Zhang, K., Hou, S., Zhou, W., and Xie, S. "Design of AgM bimetallic alloy nanostructures (M= Au, Pd, Pt) with tunable morphology and peroxidase-like activity", *Chem. Mater.*, **22**(9), pp. 2988–2994 (2010).
24. Gao, M., Lu, X., Chi, M., Chen, S., and Wang, C. "Fabrication of oxidase-like hollow $MnCo_2O_4$ nanofibers and their sensitive colorimetric detection of sulfite and l-cysteine", *Inorg. Chem. Front.*, **4**(11), pp. 1862–1869 (2017).
25. Dong, J., Song, L., Yin, J.J., He, W., Wu, Y., Gu, N., and Zhang, Y. "Co_3O_4 nanoparticles with multi-enzyme activities and their application in immunohistochemical assay", *ACS Appl. Mater. Interfaces*, **6**(3), pp. 1959–1970 (2014).
26. Yuan, F., Zhao, H., Zang, H., Ye, F., and Quan, X. "Three-dimensional graphene supported bimetallic

nanocomposites with DNA regulated-flexibly switchable peroxidase-like activity", *ACS Appl. Mater. Interfaces*, **8**(15), pp. 9855–9864 (2016).

27. Wang, H., Li, S., Si, Y., Zhang, N., Sun, Z., Wu, H., and Lin, Y. "Platinum nanocatalysts loaded on graphene oxide-dispersed carbon nanotubes with greatly enhanced peroxidase-like catalysis and electrocatalysis activities", *Nanoscale*, **6**(14), pp. 8107–8116 (2014).
28. Golchin, J., Golchin, K., Alidadian, N., Ghaderi, S., Eslamkhah, S., Eslamkhah, M., and Akbarzadeh, A. "Nanozyme applications in biology and medicine: an overview", *Artif. Cells Nanomed. Biotechnol.*, **45**(6), pp. 1069–1076 (2017).
29. Yang, B., Li, J., Deng, H., and Zhang, L. "Progress of mimetic enzymes and their applications in chemical sensors", *Crit. Rev. Anal. Chem.*, **46**(6), pp. 469–481 (2016).
30. Wang, X., Hu, Y., and Wei, H. "Nanozymes in bionanotechnology: from sensing to therapeutics and beyond", *Inorg. Chem. Front.*, **3**(1), pp. 41–60 (2016).
31. Wang, Q., Zhang, X., Huang, L., Zhang, Z., and Dong, S. "One-pot synthesis of Fe_3O_4 nanoparticle loaded 3D porous graphene nanocomposites with enhanced nanozyme activity for glucose detection", *ACS Appl. Mat. Interfaces*, **9**(8), pp. 7465–7471 (2017).
32. Lin, L., Song, X., Chen, Y., Rong, M., Zhao, T., Wang, Y., Jiang, Y., and Chen, X. "Intrinsic peroxidase-like catalytic activity of nitrogen-doped graphene quantum dots and their application in the colorimetric detection of H_2O_2 and glucose", *Anal. Chim. Acta*, **869**, pp. 89–95 (2015).
33. Li, W., Zhi, X., Yang, J., Zhang, J., and Fu, Y. "Colorimetric detection of cysteine and homocysteine based on an oligonucleotide-stabilized Pd nanozyme", *Anal. Methods*, **8**(25), pp. 5111–5116 (2016).
34. Zhang, D., Chen, Z., Omar, H., Deng, L., and Khashab, N.M. "Colorimetric peroxidase mimetic assay for uranyl detection in sea water", *ACS Appl. Mater. Interfaces*, **7**(8), pp. 4589–4594 (2015).
35. Sahoo, R., Santra, S., Ray, C., Pal, A., Negishi, Y., Ray, S.K., and Pal, T. "Hierarchical growth of $ZnFe_2O_4$ for sensing applications", *New J. Chem.*, **40**(2), pp. 1861–1871 (2016).
36. Jia, H., Yang, D., Han, X., Cai, J., Liu, H., and He, W. "Peroxidase-like activity of the Co_3O_4 nanoparticles used for biodetection and evaluation of antioxidant behavior", *Nanoscale*, **8**(11), pp. 5938–5945 (2016).
37. Jin, C., Lu, F., Cao, X., Yang, Z., and Yang, R. "Facile synthesis and excellent electrochemical properties of $NiCo_2O_4$ spinel nanowire arrays as a bifunctional catalyst for the oxygen reduction and evolution reaction", *J. Mater. Chem. A*, **1**(39), pp. 12170–12177 (2013).
38. Vetr, F., Moradi-Shoeili, Z., and Özkar, S. "Mesoporous $MnCo_2O_4$ with efficient peroxidase mimetic activity for detection of H_2O_2", *Inorg. Chem. Commun.*, **98**, pp. 184–191 (2018).
39. Vetr, F., Moradi-Shoeili, Z., and Özkar, S. "Oxidation of o-phenylenediamine to 2, 3-diaminophenazine in the presence of cubic ferrites MFe_2O_4 (M= Mn, Co, Ni, Zn) and the application in colorimetric detection of H_2O_2", *Appl. Organomet. Chem.*, **32**(9), p. e4465 (2018).
40. Leal, E., Dantas, J., dos Santos, P.T.A., Bicalho, S.M.D.C.M., Kiminami, R.H.G.A., da Silva, M.R., and de Melo Costa, A.C.F. "Effect of the surface treatment on the structural, morphological, magnetic and biological properties of MFe_2O_4 iron spinels (M= Cu, Ni, Co, Mn and Fe)", *Appl. Surf. Sci.*, **455**, pp. 635–645 (2018).
41. Su, L., Qin, W., Zhang, H., Rahman, Z.U., Ren, C., Ma, S., and Chen, X. "The peroxidase/catalase-like activities of MFe_2O_4 (M= Mg, Ni, Cu) MNPs and their application in colorimetric biosensing of glucose", *Biosens. Bioelectron.*, **63**, pp. 384–391 (2015).
42. Wang, T., Su, P., Li, H., Yang, Y., and Yang, Y. "Triple-enzyme mimetic activity of Co_3O_4 nanotubes and their applications in colorimetric sensing of glutathione", *New J. Chem.*, **40**(12), pp. 10056–10063 (2016).
43. Zhu, X., Zhao, H., Niu, X., Liu, T., Shi, L. and Lan, M. "A comparative study of carbon nanotube supported MFe_2O_4 spinels (M= Fe, Co, Mn) for amperometric determination of H_2O_2 at neutral pH values", *Microchim. Acta*, **183**(8), pp. 2431–2439 (2016).
44. Hutchings, G.J., Mirzaei, A.A., Joyner, R.W., Siddiqui, M.R.H., and Taylor, S.H. "Effect of preparation conditions on the catalytic performance of copper manganese oxide catalysts for CO oxidation", *Appl. Catal. A*, **166**(1), pp. 143–152 (1998).
45. Hall, B.D., Zanchet, D., and Ugarte, D. "Estimating nanoparticle size from diffraction measurements", *J. Appl. Crystallogr.*, **33**(6), pp. 1335–1341(2000).
46. Saravanakumar, B., Lakshmi, S.M., Ravi, G., Ganesh, V., Sakunthala, A., and Yuvakkumar, R. "Electrochemical properties of rice-like copper manganese oxide ($CuMn_2O_4$) nanoparticles for pseudocapacitor applications", *J. Alloys Compd*, **723**, pp. 115–122 (2017).
47. Lin, T., Zhong, L., Song, Z., Guo, L., Wu, H., Guo, Q., Chen, Y., Fu, F., and Chen, G. "Visual detection of blood glucose based on peroxidase-like activity of WS_2 nanosheets", *Biosens. Bioelectron.*, **62**, pp. 302–307 (2014).
48. Guan, J., Peng, J., and Jin, X. "Synthesis of copper sulfide nanorods as peroxidase mimics for the colorimetric detection of hydrogen peroxide", *Anal. Methods*, **7**(13), pp. 5454–5461 (2015).
49. Chen, W., Chen, J., Liu, A.L., Wang, L.M., Li, G.W., and Lin, X.H. "Peroxidase-like activity of cupric oxide nanoparticle", *Chem. Cat. Chem.*, **3**(7), pp. 1151–1154 (2011).
50. Maddinedi, S.B. and Mandal, B.K. "Peroxidase Like activity of quinic acid stabilized copper oxide nanosheets", *Austin J. Anal. Pharm. Chem.*, **1**(2), p. 4 (2014).

51. Wang, X., Han, Q., Cai, S., Wang, T., Qi, C., Yang, R., and Wang, C. "Excellent peroxidase mimicking property of CuO/Pt nanocomposites and their application as an ascorbic acid sensor", *Analyst*, **142**(13), pp. 2500–2506 (2017).

52. Nimse, S.B. and Pal, D. "Free radicals, natural antioxidants, and their reaction mechanisms", *Rsc Adv.*, **5**(35), pp. 27986–28006 (2015).

53. Shah, J., Purohit, R., Singh, R., Karakoti, A.S., and Singh, S. "ATP-enhanced peroxidase-like activity of gold nanoparticles", *J. Colloid. Interface Sci.*, **456**, pp. 100–107 (2015).

54. Huang, W., Lin, T., Cao, Y., Lai, X., Peng, J., and Tu, J. "Hierarchical $NiCo_2O_4$ hollow sphere as a peroxidase mimetic for colorimetric detection of H_2O_2 and glucose", *Sensors*, **17**(1), p. 217 (2017).

55. Chen, W., Cai, S., Ren, Q.Q., Wen, W., and Zhao, Y.D. "Recent advances in electrochemical sensing for hydrogen peroxide: a review", *Analyst*, **137**(1), pp. 49–58 (2012).

56. Pundir, C.S., Deswal, R., and Narwal, V. "Quantitative analysis of hydrogen peroxide with special emphasis on biosensors", *Bioproc. Biosyst. Eng.*, **41**(3), pp. 313–329 (2018).

57. Rhee, S.G., Chang, T.S., Jeong, W., and Kang, D. "Methods for detection and measurement of hydrogen peroxide inside and outside of cells", *Mol. Cells*, **29**(6), pp. 539–549 (2010).

58. Sun, Y., Wang, J., Li, W., Zhang, J., Zhang, Y., and Fu, Y. "DNA-stabilized bimetallic nanozyme and its application on colorimetric assay of biothiols", *Biosens. Bioelectron.*, **74**, pp. 1038–1046 (2015).

59. Yang, Y.K., Shim, S., and Tae, J. "Rhodamine-sugar based turn-on fluorescent probe for the detection of cysteine and homocysteine in water", *Chem. Commun.*, **46**(41), pp. 7766–7768 (2010).

60. Shahrokhian, S. "Lead phthalocyanine as a selective carrier for preparation of a cysteine-selective electrode", *Anal. Chem.*, **73**(24), pp. 5972–5978 (2001).

61. Chen, Y., Chen, T., Wu, X., and Yang, G. "$CuMnO_2$ nanoflakes as pH-switchable catalysts with multiple enzyme-like activities for cysteine detection", *Sens. Actuators B*, **279**, pp. 374–384 (2019).

62. Chi, M., Zhu, Y., Jing, L., Wang, C., and Lu, X. "Fabrication of ternary MoS_2-polypyrrole-Pd nanotubes as peroxidase mimics with a synergistic effect and their sensitive colorimetric detection of l-cysteine", *Anal. Chim. Acta*, **1035**, pp. 146–153 (2018).

63. Chen, S., Chi, M., Zhu, Y., Gao, M., Wang, C., and Lu, X. "A facile synthesis of superparamagnetic Fe_3O_4 nanofibers with superior peroxidase-like catalytic activity for sensitive colorimetric detection of l-cysteine", *Appl. Surf. Sci.*, **440**, pp. 237–244 (2018).

64. Li, Y., Zhang, Z., Tao, Z., Gao, X., Wang, S., and Liu, Y. "A Asp/Ce nanotube-based colorimetric nanosensor for H_2O_2-free and enzyme-free detection of cysteine", *Talanta*, **196**, pp. 556–562 (2019).

Biographies

Monir Rahnamabaghy received her BS degree in Pure Chemistry from Tabriz University, Tabriz, Iran, and her MS degree in the field of Crystal Growth, in 2007, from Imam Khomeini International University, Qazvin, Iran, under the supervision of Professor S. Gammamy. Currently, she is a PhD candidate in Professor Abdollah Fallah Shojaei's group at Guilan University. Her research interests are focused on the synthesis of new nanozymes and study of their wide applications in biomedicine and bioanalysis.

Abdollah Fallah Shojaei received his BS degree in Applied Chemistry from Tehran University, Tehran, Iran, in 1991. Following a 3 year MS degree research experience in the group of Professor Morteza Famil Farnia (Department of Chemistry, Tehran University), working on the synthesis of zinc and cadmium complexes of 1,4 diaza 1,3 butadianes, he received his PhD degree from Isfahan University, Isfahan, Iran, in 2005. He worked with a group supervised by Professor Mohammad Hossien Habibi and Professor Shahram Tangestaninejad to study photolytic recovery of inorganic mercury compounds. He is currently Professor in the Department of Chemistry at the University of Guilan, Iran. His research interests include synthesis, characterization, photocatalytic, and sensor properties of nanocomposites.

Zeinab Moradi-Shoeili obtained her PhD degree in Inorganic Chemistry from Sharif University of Technology, Tehran, Iran, under the supervision of Professor Davar M. Boghaei, in 2013. She is currently Associate Professor of Inorganic Chemistry at the University of Guilan, Iran. Her main areas of interest include biomimetic catalytic systems and their applications in sensors and biosensors, synthesis of novel homogeneous and heterogeneous catalysts for oxidation reactions, and bionanomaterials.